

# Supporting information

## **In-situ carbon coated flower-like VPO<sub>4</sub> as an anode material for potassium-ion batteries**

Jiaying Liao, Qiao Hu, Jinxiao Mu, Xiaodong He, Shuo Wang, Jiemin Dong, Chunhua Chen\*

*CAS Key Laboratory of Materials for Energy Conversions, Department of Materials Science and Engineering & Collaborative Innovation Center of Suzhou Nano Science and Technology, University of Science and Technology of China, Hefei 230026, Anhui, China*

## Experimental section

### *Materials synthesis*

**VOPO<sub>4</sub>·2H<sub>2</sub>O** was prepared by a typical reflux method [S1]. 9.6 g V<sub>2</sub>O<sub>5</sub> and 50 ml H<sub>3</sub>PO<sub>4</sub> (85%) were added to 200 ml deionized water, and then refluxed at 110 °C for 6 h. The resulting yellow precipitate was collected by filtration, washed with cold water and acetone, then dried in a vacuum oven at 80 °C.

**VOHPO<sub>4</sub>·0.5H<sub>2</sub>O** was prepared from the direct reduction of VOPO<sub>4</sub>·2H<sub>2</sub>O [S2]. 4 g VOPO<sub>4</sub>·2H<sub>2</sub>O was dispersed in 100 ml isobutanol and refluxed at 110 °C for 8 h. A light blue precipitate was collected by filtration, washed with ethanol and denoted as VOHPO<sub>4</sub>-B.

**VOHPO<sub>4</sub>·yC<sub>4</sub>H<sub>9</sub>OH**: 4 g VOPO<sub>4</sub>·2H<sub>2</sub>O was dispersed in 100 ml isobutanol and stirred at room temperature for 12 h to intercalate isobutanol into the VOPO<sub>4</sub> layers. Then the intermediate product was heated stepwise at 30 °C, 50 °C and 70 °C for 1h, respectively. Finally, it was refluxed at 110 °C for 8 h. The resulting precipitate was denoted as VOHPO<sub>4</sub>-F.

**VPO<sub>4</sub>**: VOPO<sub>4</sub>·2H<sub>2</sub>O, VOHPO<sub>4</sub>-B and VOHPO<sub>4</sub>-F were annealed at 800 °C under a mixed H<sub>2</sub>/Ar (5%) reduction atmosphere for 2 h, and the as-obtained VPO<sub>4</sub> samples were marked as VPO<sub>4</sub>-P, VPO<sub>4</sub>-B and VPO<sub>4</sub>-F, respectively.

### *Characterization*

The phases of as-obtained products were characterized with an X-ray diffractometer (Rigaku TTR-III, Cu K $\alpha$  radiation). The morphology of the samples was studied with a scanning electron microscope (SEM, FEI Apreo) and a transmission electron microscope (TEM, JEM-2100F). The elemental mappings were analyzed by energy dispersive X-ray spectroscopy (EDS) attached to the SEM instrument. Thermogravimetric analysis (TGA) was performed at a heating rate of 10 °C min<sup>-1</sup> in the temperature range of 25-800 °C under air atmosphere (DTG-60H, Shinadzu). The carbon contents were also measured with an Infrared Carbon-sulfur analyzer (CS-8800C, Jinbo). The specific surface area was measured by N<sub>2</sub>-adsorption/desorption

(ASAP 2020). Raman spectra (Renishaw inVia Raman Microscope) were recorded on the condition of 532 nm diode laser excitation. Fourier transformation infrared spectroscopy (FTIR, Magna-IR 750 spectrometer) in the range of 400-4000  $\text{cm}^{-1}$  was performed.

#### *Electrochemical evaluation*

The  $\text{VPO}_4$  electrodes consisted of the active material (70 wt. %), acetylene black (20 wt. %) and carboxymethyl cellulose binder (10 wt. %) on copper foil. The typical  $\text{VPO}_4$  mass loadings were about 1.5  $\text{mg cm}^{-2}$ , respectively. The electrochemical properties of the obtained materials were evaluated in coin-type cells (CR2032 size), which were assembled in an argon filled glove box (MBraun Unilab). For the fabrication of potassium half cells, potassium metal was used as the counter electrode, 3  $\text{mol L}^{-1}$  KFSI in DME was used as the electrolyte and a Whatman glass-fiber separator was used. The cells were galvanostatically cycled on a multi-channel battery test system (Neware BTS-2300, Shenzhen) in the voltage range of 0.01-3.0 V. The cyclic voltammetry (CV) of the cells was conducted on a CHI 660C electrochemical workstation at the scan rate of 0.1-2.0  $\text{mV s}^{-1}$ . The electrochemical impedance spectra (EIS) were measured through a frequency range between 0.01 Hz to 100 kHz.

#### *Ex-situ measurements*

The cells were charged and discharged at a low current of 50  $\text{mA g}^{-1}$  to a certain voltage, and then were disassembled and washed by DME in the glove box. Polyimide films are covered at the surface of electrodes in glove box before the ex-situ XRD test.

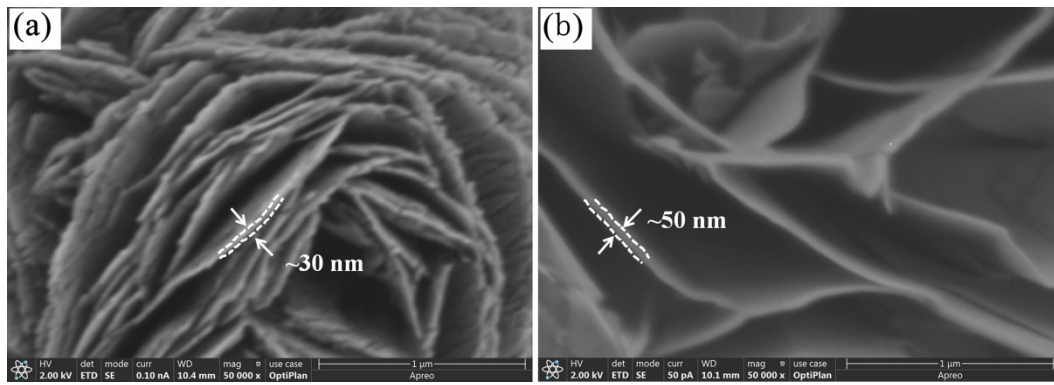


**Fig. S1** SEM images of VPO<sub>4</sub>-B (a) and VPO<sub>4</sub>-F (b).

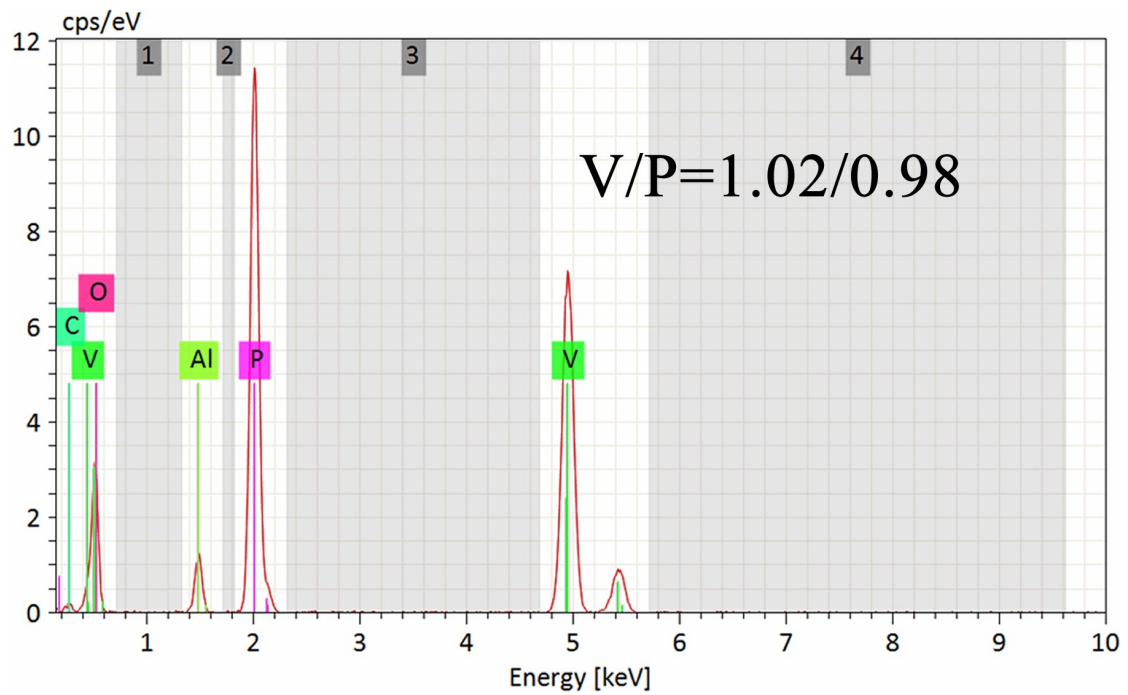


**Fig. S2** EDS result of VPO<sub>4</sub>-F.

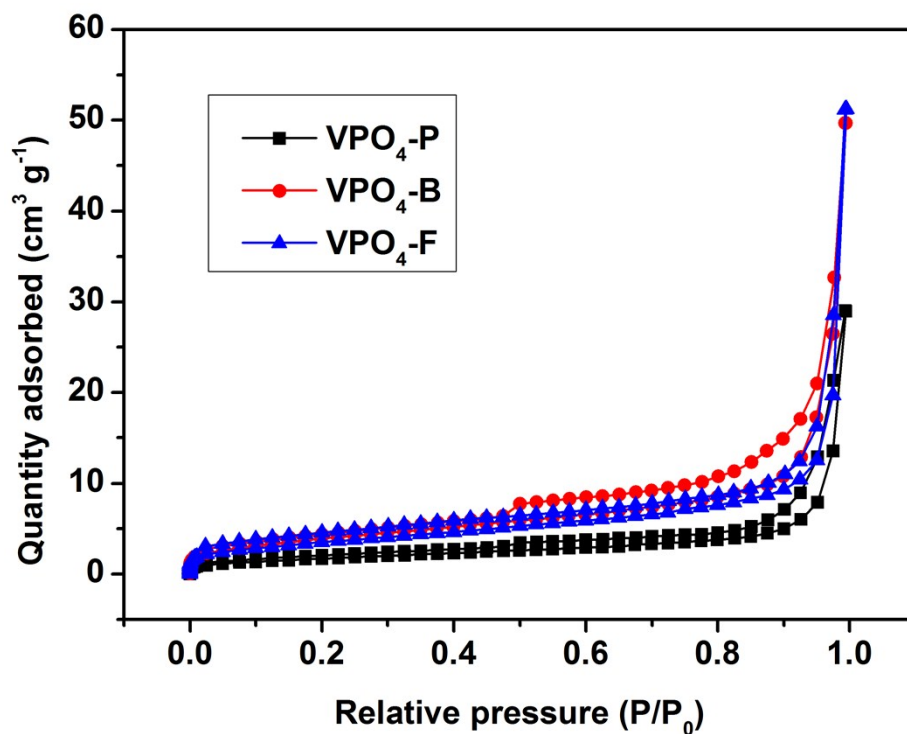


Fig. S3 N<sub>2</sub> adsorption-desorption isotherms of VPO<sub>4</sub> samples.

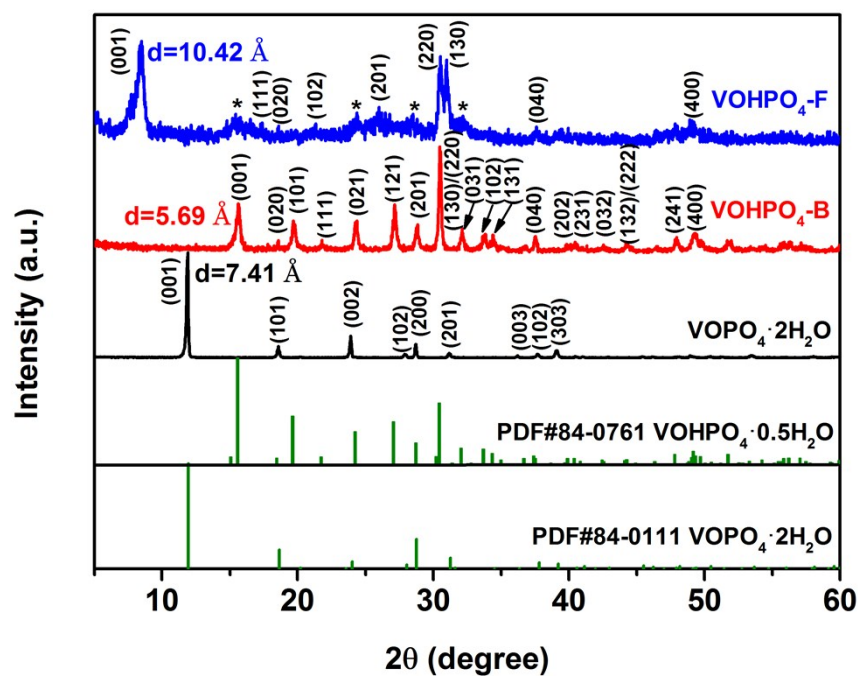


Fig. S4 XRD patterns of VOPO<sub>4</sub>·2H<sub>2</sub>O and VOHPO<sub>4</sub>. A small amount of un-intercalated VOHPO<sub>4</sub>·0.5H<sub>2</sub>O in VOHPO<sub>4</sub>-F is marked with asterisk (\*).

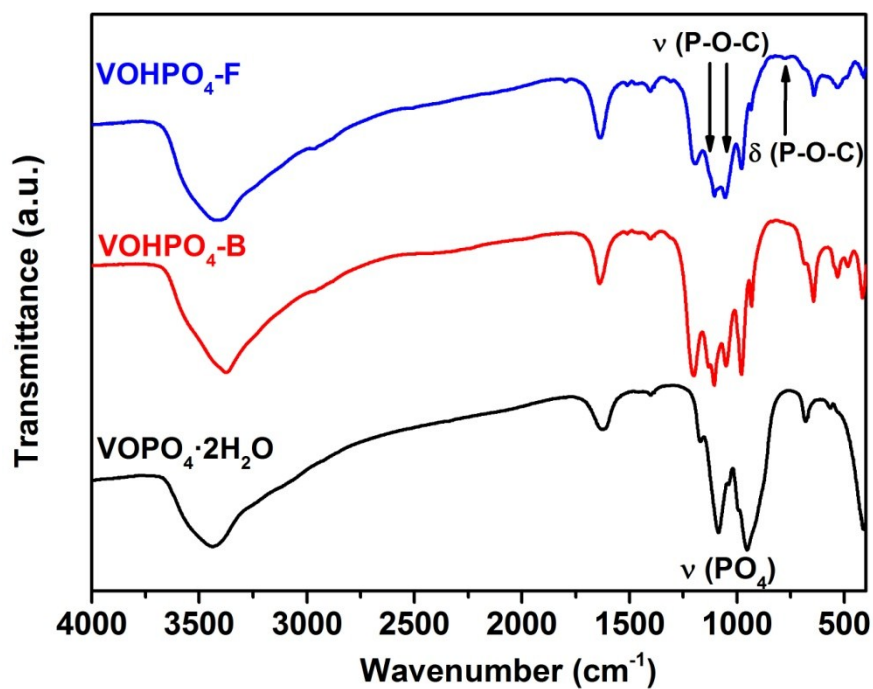


Fig. S5 FTIR spectra of  $\text{VOPO}_4 \cdot 2\text{H}_2\text{O}$  and  $\text{VOHPO}_4$ .

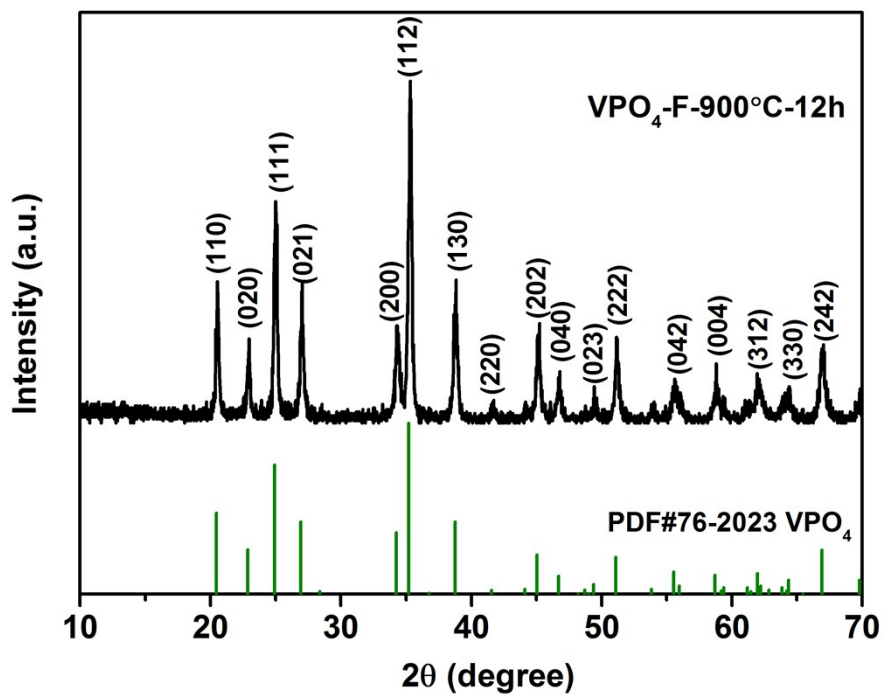


Fig. S6 XRD patterns of  $\text{VOHPO}_4\text{-F}$  after annealing in  $\text{H}_2/\text{Ar}$  at  $900^\circ\text{C}$  for 12h.

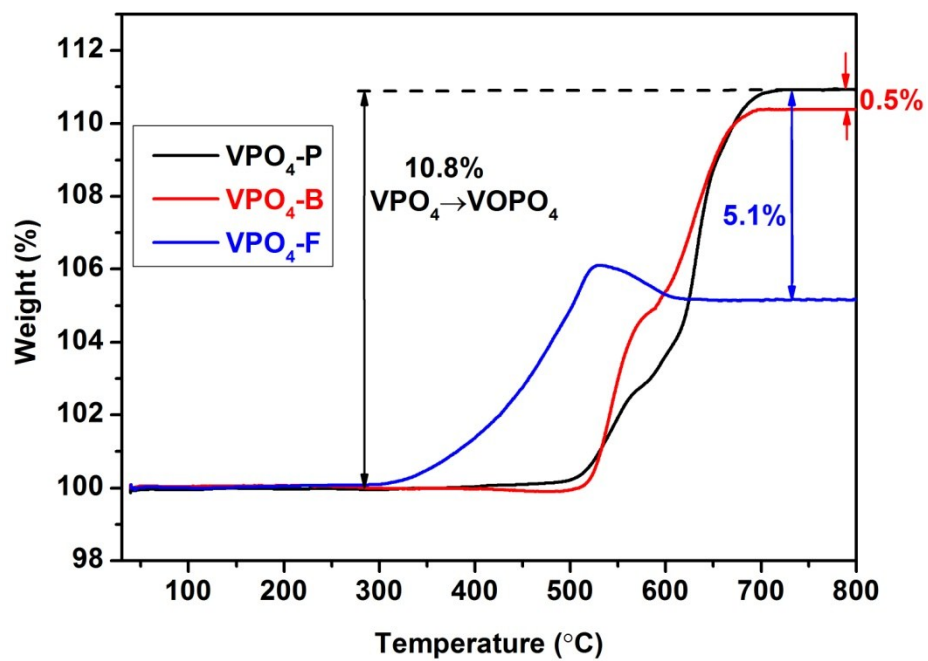


Fig. S7 TG curves of VPO<sub>4</sub> samples.

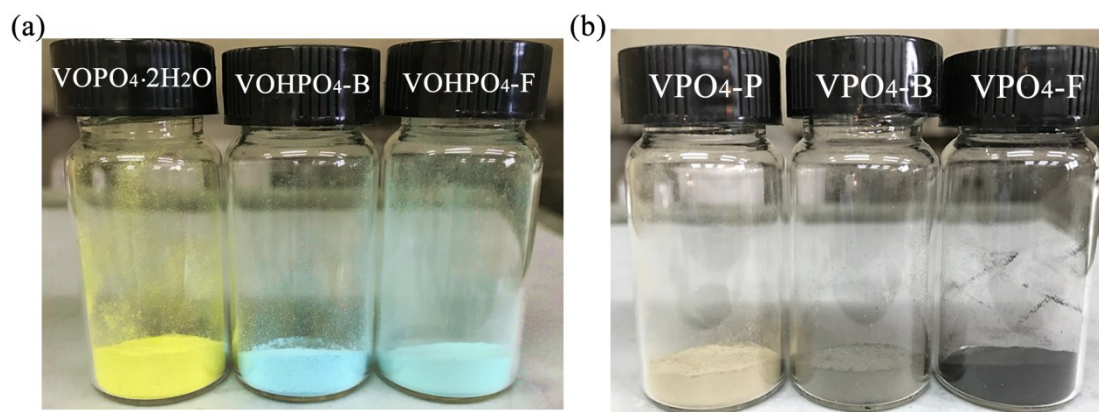


Fig. S8 Optical photographs of VOPO<sub>4</sub>·2H<sub>2</sub>O and VOHPO<sub>4</sub> (a), VPO<sub>4</sub> samples (b).

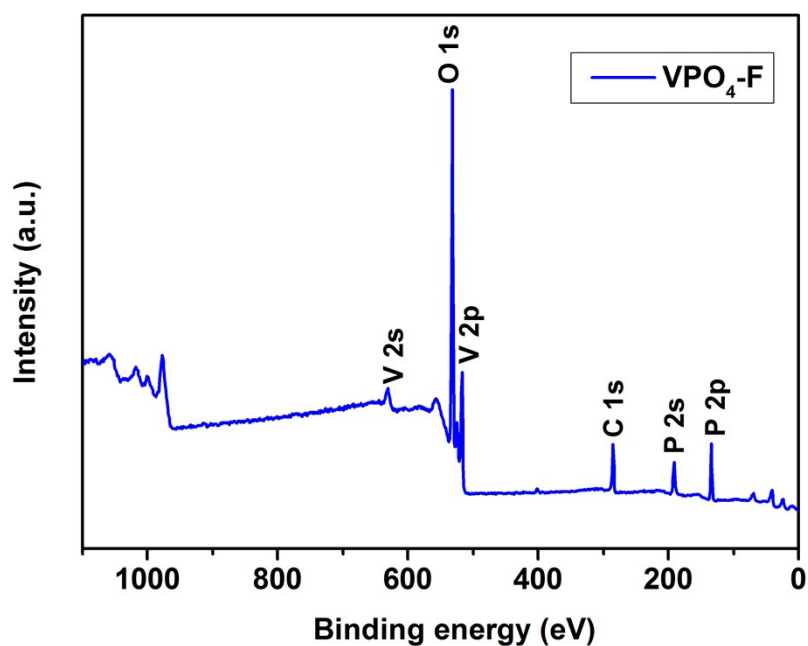


Fig. S9 XPS spectrum of VPO<sub>4</sub>-F.

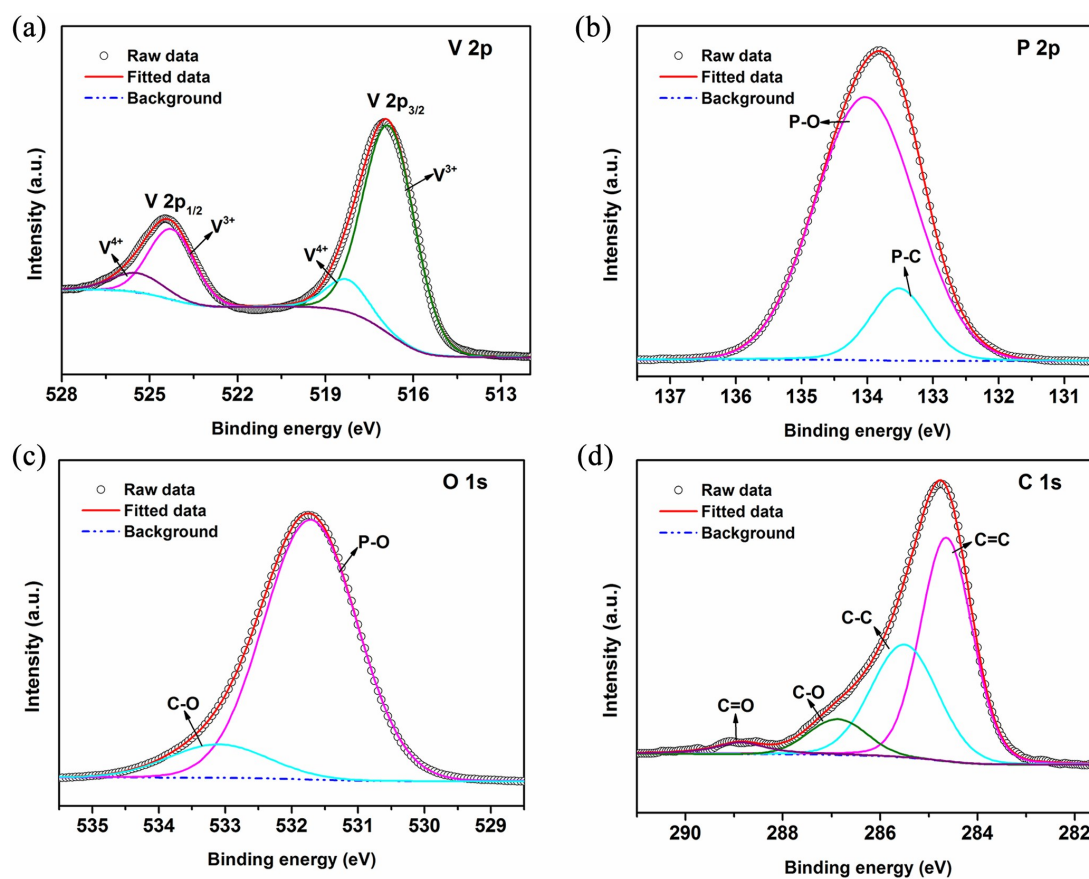
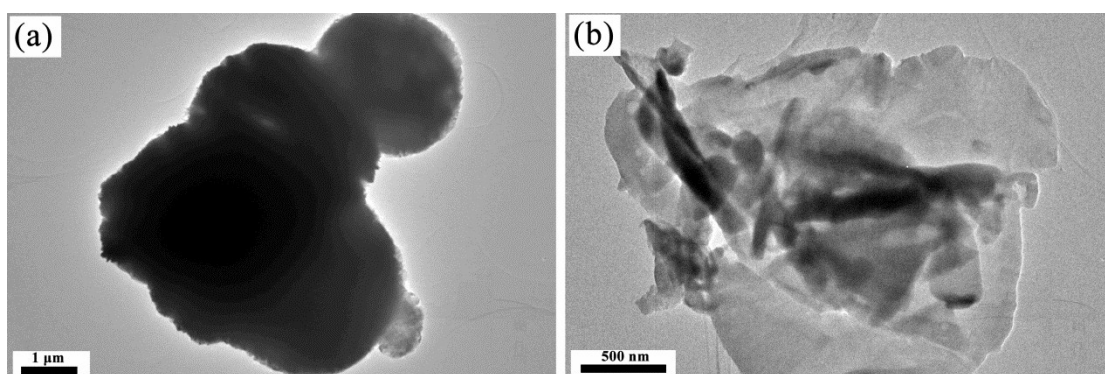
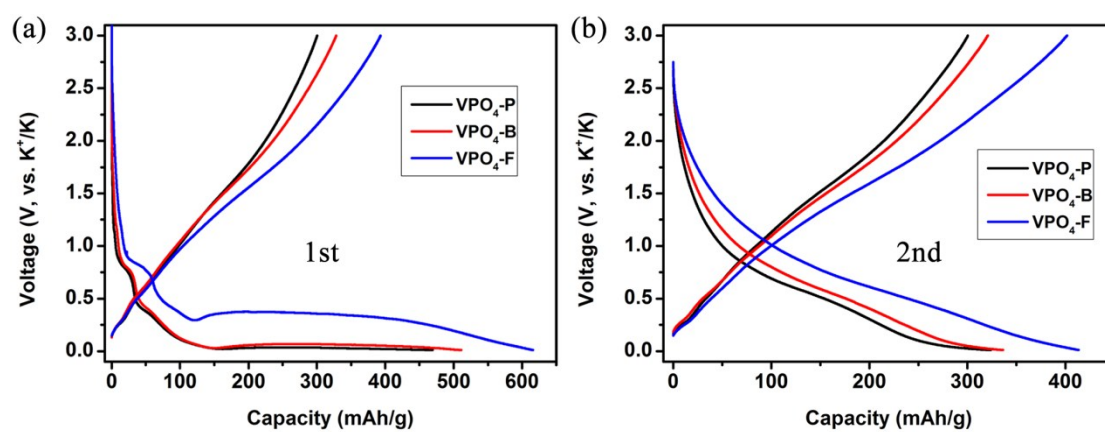


Fig. S10 High-resolution XPS spectra of V 2p (a), P 2p (b), O 1s (c), and C 1s (d) of VPO<sub>4</sub>-F.



**Fig. S11** TEM images of VPO<sub>4</sub>-B (a) and VPO<sub>4</sub>-F (b).



**Fig. S12** The comparison of the 1<sup>st</sup> (a) and the 2<sup>nd</sup> (b) discharge/charge curves of the VPO<sub>4</sub> samples at a current density of 50 mA g<sup>-1</sup>.

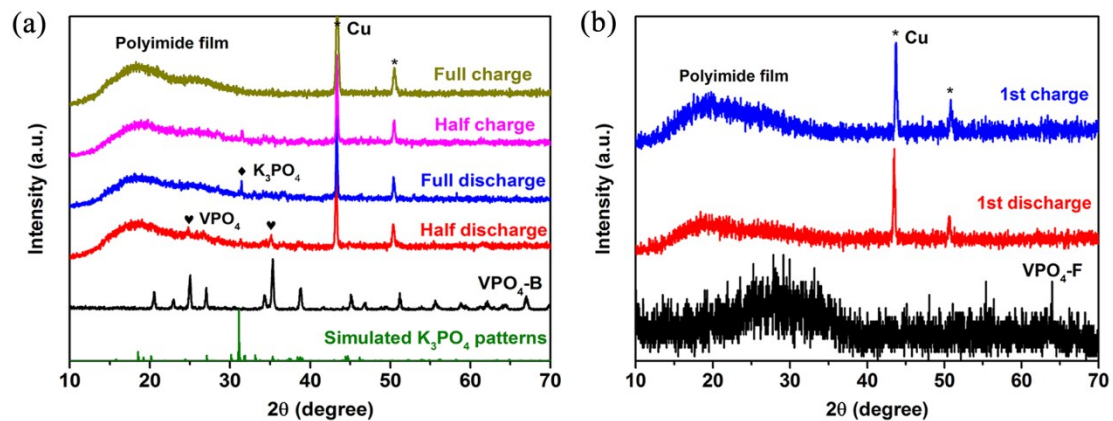


**Fig. S13** *Ex-situ* XRD patterns of crystalline  $VPO_4-B$  (a) and amorphous  $VPO_4-F$  (b) at different discharge/charge states of the 1<sup>st</sup> cycle.

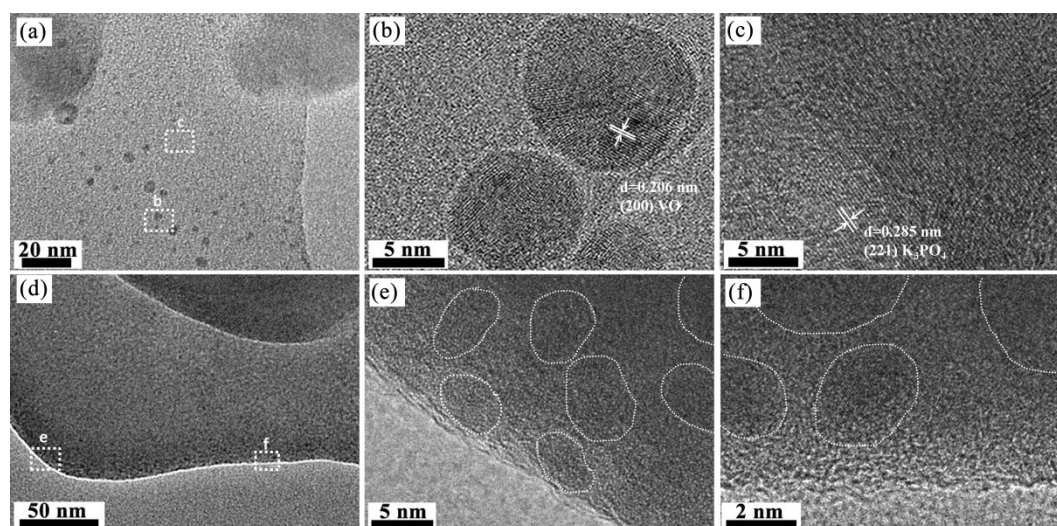


**Fig. S14** TEM and HR-TEM images of  $VPO_4-B$  (a-c) and  $VPO_4-F$  (d-f) electrodes after the 1<sup>st</sup> discharge process.

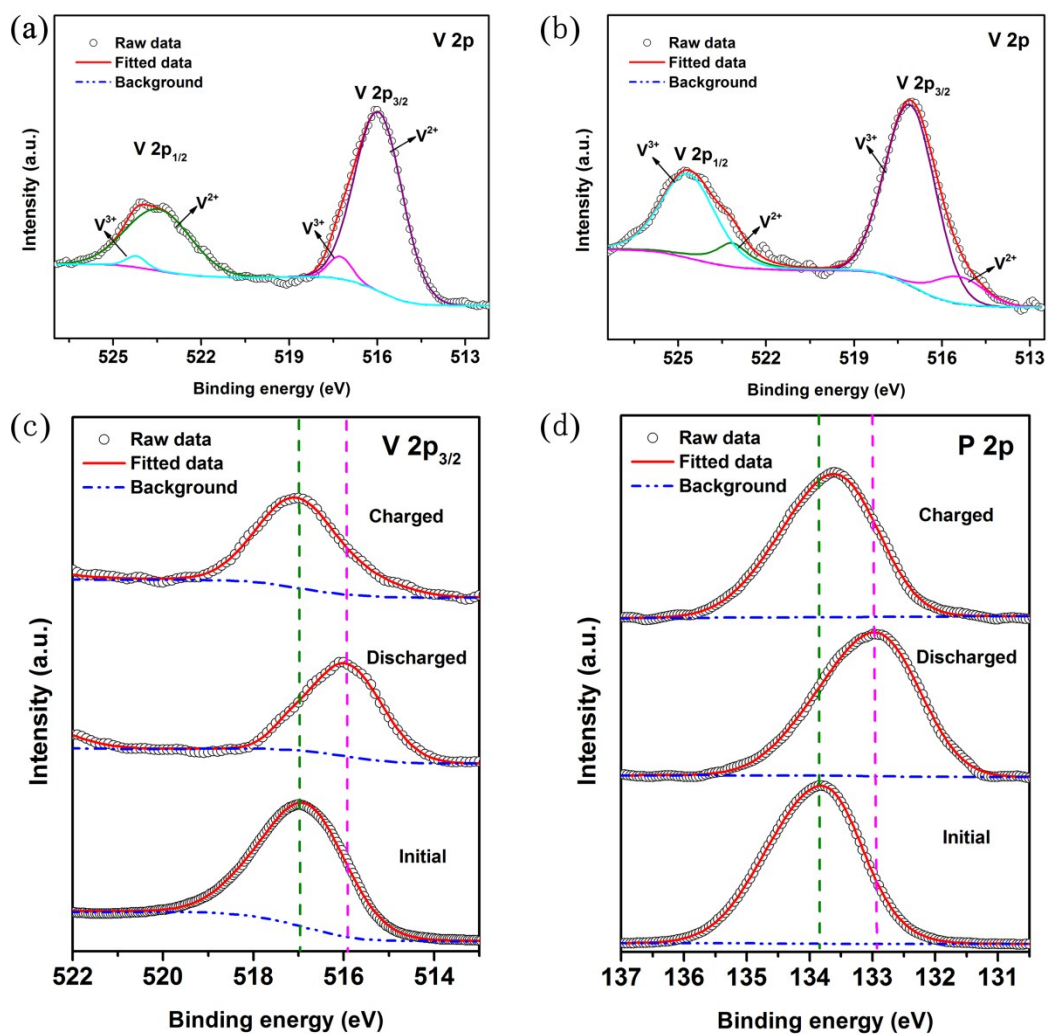


**Fig. S15** High-resolution XPS spectra of V 2p at the 1<sup>st</sup> discharged (a) and charged (b) states of VPO<sub>4</sub>-F. V 2p (c) and P 2p (d) XPS spectra of VPO<sub>4</sub>-F at different electrochemical stages.

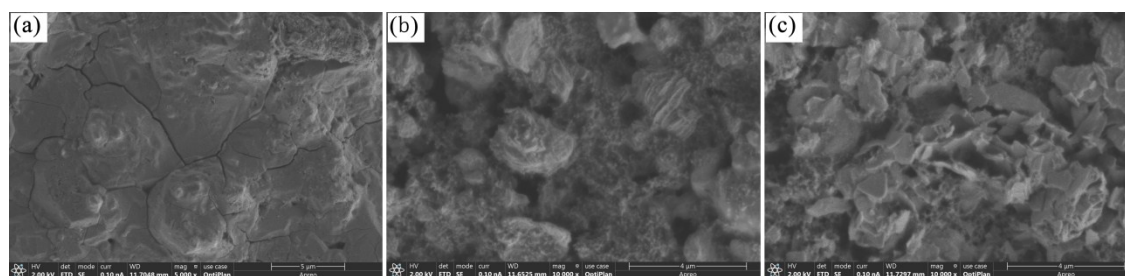


**Fig. S16** SEM images of the electrodes after 100 cycles: (a) VPO<sub>4</sub>-P, (b) VPO<sub>4</sub>-B, (c) VPO<sub>4</sub>-F.

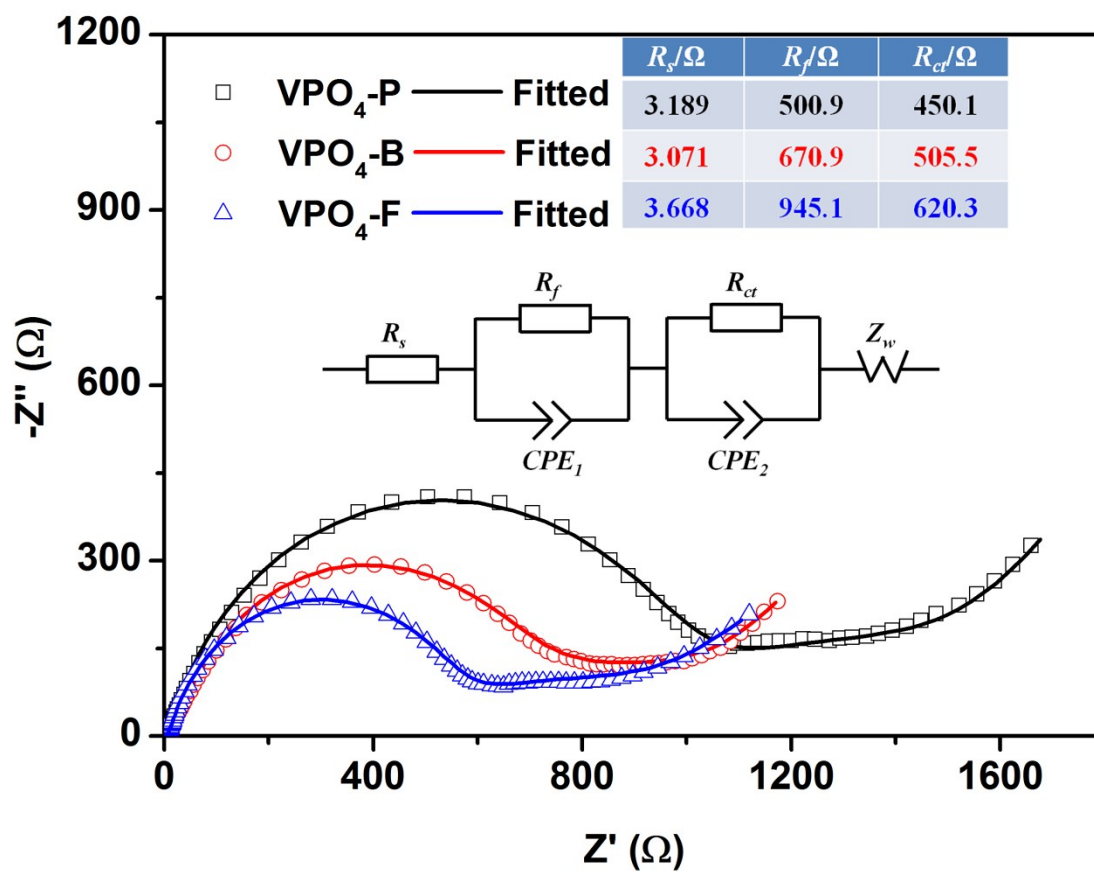
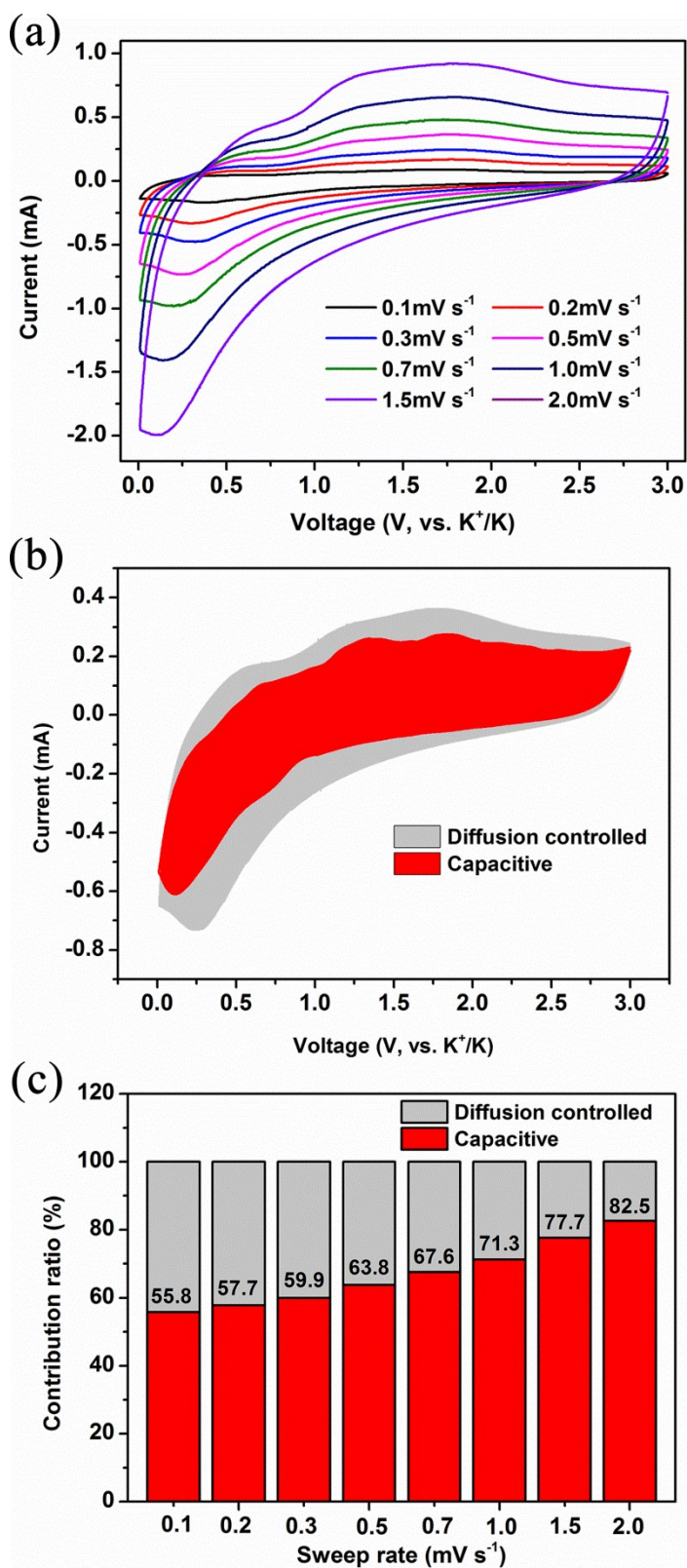


Fig. S17 EIS spectra of VPO<sub>4</sub> samples fitted using the inset equivalent electrical circuit model. The cells were first discharged to 0.01 V and charged to 2.0 V.



**Fig. S18** (a) CV curves of VPO<sub>4</sub>-F at various sweep rates from 0.1 to 2.0 mV s<sup>-1</sup>; (b) Separation of the capacitive and diffusion-controlled currents at a sweep rate of 0.5 mV s<sup>-1</sup>; (c) Contribution ratio of the capacitive and diffusion-controlled charge at various sweep rates.

## References

[S1] H. R. Tietze, *Aust. J. Chem* **1981**, 34, 2035.

[S2] N. Yamamoto, N. Hiyoshi and Toshio Okuhara, *Chem. Mater.* **2002**, 14, 3882.